Available online at www.sciencedirect.com
ScienceDirect
Trans. Nonferrous Met. Soc. China 23(2013) 1334−1341
Transactions of Nonferrous Metals Society of China
www.tnmsc.cn

Preparation, characterization and electrochemical properties of boron-doped diamond films on Nb substrates

Zhi-ming YU[1,2], Jian WANG[1], Qiu-ping WEI[1,2], Ling-cong MENG[1], Shi-meng HAO[1], Fen LONG[1]

1. School of Materials Science and Engineering, Central South University, Changsha 410083, China;
2. State Key Laboratory of Powder Metallurgy, Central South University, Changsha 410083, China

Received 10 April 2012; accepted 15 November 2012

Abstract: A series of boron-doped polycrystalline diamond films were prepared by hot filament (HF) chemical vapor deposition on Nb substrates. The effects of B/C ratio of reaction gas on film morphology, growth rate, chemical bonding states, phase composition and electrochemical properties of each deposited sample were studied by scanning electron microscopy, Raman spectra, X-ray diffraction, microhardness indentation, and electrochemical analysis. Results show that the average grain size of diamond and the growth rate decrease with increasing the B/C ratio. The diamond films exhibit excellent adhesion under Vickers microhardness testing (9.8 N load). The sample with 2% B/C ratio has a wider potential window and a lower background current as well as a faster redox reaction rate in H_2SO_4 solution and $KFe(CN)_6$ redox system compared with other doping level electrodes.

Key words: diamond film; hot filament chemical vapor deposition (HFCVD); boron doping; electrochemical behavior; niobium substrate; electrode

1 Introduction

Diamond possesses many unique physical and chemical properties as an excellent candidate for high-frequency and high-power electronics, such as high breakdown voltage, high electron and hole mobilities, negative electron affinity and stable chemical properties [1,2]. However, the extremely high inherent electrical resistivity of natural diamond, with a bandgap of 5.47 eV, restricts its application in electric devices, especially when it is used as an electrode material. This problem can be resolved by the p-doping with boron which introduces ‘midgap’ states to enhance conductivity and electron-transfer reactivity of diamond films [3]. Elevating the boron doping level can convert insulating diamond films into metallic ones [4]. Additionally, superconductivity in diamond films can be obtained at very high doping levels [5,6].

Recently, diamond electrodes have attracted considerable interest due to their excellent electrochemical properties. Compared with the conventional electrodes, boron-doped diamond (BDD) thin-film electrodes have a wide electrochemical potential window, a very low voltammetric background current, a high resistance to deactivation by fouling, a very high electrochemical stability and a relative insensitivity to dissolved oxygen [7]. It is hoped that BDD films are new promising electrode materials for the field of electroanalysis [8], electrosynthesis [9] and water treatment [10].

During the past 10 years, many studies on boron-doping and electrochemical characteristics have been reported for boron-doped diamond films [11,12]. Most of the reported doped diamond films were deposited onto p-type silicon wafers [13,14]. It is known that because of the similar sp^3 crystal structure and SiC transition layer between diamond and silicon, highly perfect and pore-free diamond films can be formed on silicon substrate. However, the brittleness and restricted conductivity of this substrate limit its use in many practical applications. When it works as an electrode, the good (ohmic contact) must be ensured between the backside of Si substrate and a metal current collector

Foundation item: Project (21271188) supported by the National Natural Science Foundation of China; Project (2012M521541) supported by the China Postdoctoral Science Foundation, China; Project (2012QNZT002) supported by the Fundamental Research Funds for the Central Universities, China; Project (20110933K) supported by the State Key Laboratory of Powder Metallurgy, China; Project (CSUZC2013016) supported by the Open-End Fund for Valuable and Precision Instruments of Central South University, China
Corresponding author: Qiu-ping WEI; Tel: +86-731-88830335; E-mail: qiupwei@csu.edu.cn
DOI: 10.1016/S1003-6326(13)62601-1

plate [13,15]. Therefore, it would be better if we choose metal substrates with good mechanical and electric properties to grow diamond films, particularly for the preparation of large-area electrodes. Among these mental materials, niobium is the most favorable because of its excellent resistance performance to acid, alkali and corrosion, which can withstand high temperature and hydrogen-containing atmospheres [3,16,17].

Boron-doping levels can greatly influence the morphology, microstructure, defect density and nondiamond carbon impurity content in diamond film, consequently, influencing the electrochemical response of the diamond thin film electrode [18,19]. It is crucial to make a systematical study on the basic characteristic of different doping level diamond films integrated with their electrochemical properties. In this work, a series of high quality boron-doped diamond films were deposited on Nb substrates via hot filament chemical vapor deposition (HFCVD) and their properties in acid electrolyte and redox-system as a function of the boron-doping level were studied.

2 Experimental

Diamond films were deposited on Nb plates using a HF assisted CVD reactor system which was designed and manufactured in the Department of Physics at the Royal Institute of Technology, Stockholm (Sweden) [20]. The flat specimens used in this study were 7 mm×7 mm×1 mm. Prior to diamond film deposition, the surface of Nb substrates was polished with 600, 800, 1200, 1600 metallographic abrasive papers to get mirror-like smoothness and eliminate the possible negative effects caused by contaminations and oxide layer. In order to increase the diamond nucleation density and quality, the substrates were subsequently mechanically scratched on a felt polishing pad with 250 nm in diameter diamond powder for 10 min. It is believed that the micro- to nano-scale diamond fragments left on the substrate during the process of agitation act as nucleation seeds upon subsequent diamond growth [21]. Then, the substrates were ultrasonically cleaned in pure acetone for 10 min to remove the polishing debris from scratches. Afterwards, they were dried by nitrogen gas and placed into a vacuum chamber immediately. The reaction gas was a mixture of 100 cm^3/min H_2 and 1 cm^3/min CH_4. Diborane (B_2H_6) gas diluted in H_2 was used as the source of B at different volume fractions, namely the B/C ratios are 0, 0.15%, 0.3%, 0.45%, 0.75%, 2%, 3%, 4%, 5%, 6%, respectively. The system pressure was maintained at 3.5 kPa. The substrate temperature measured with two thermocouples attached to opposite edges of the substrate was about 800 °C and the growth time was 6 h.

The surface morphology, roughness and cross-sectional thickness of the as-grown diamond films were characterized by field-emission scanning electron microscopy (FE-SEM FEI, Sirion200) and atomic force microscopy (AFM NT-MDT, Solver P47). The diamond quality and bonding structures were assessed by Raman spectroscopy (LabRAM HR800), at an excitation wavelength of 488 nm (argon ion laser, output power of 100 mW) with a typical resolution of 1−2 cm^{-1} in the back-scattering geometry with a spot size of about 2 μm. The phase transformation was analyzed by X-ray diffraction (XRD: Dmax−2500VBX using Cu K_α radiation at a wavelength of 0.154 nm). Cyclic voltammetric (CV) measurements were performed on an IM6eX (ZAHNER, Germany) electrochemical station. In these CV experiments, only the side of electrode coated with diamond film was studied, so the remainder of the electrode was carefully encapsulated within insulated epoxy, to prevent edge from conduction or charge from passage through the rear of the electrode. The geometric area of the diamond in contact with the electrolyte was about 0.49 cm^2. The counter electrode was a platinum foil, and the reference electrode was a saturated calomel electrode. All potentials were reported with respect to the calomel reference electrode (SCE). 1 mol/L H_2SO_4 solution was used to study the potential window and background current. 0.1 mol/L KCl+0.01 mol/L $KFe(CN)_6$ redox system was used to research the electrode kinetics and reactions. The electrochemical data were obtained using electrodes that had been exposed to the laboratory atmosphere for several weeks.

3 Results and discussion

Figure 1 shows the SEM images of diamond films deposited under various B/C ratios in comparison with the undoped diamond films. It is clear that the diamond grain size (1−2 μm) does not change obviously when the B/C ratio is in the range of 0−2%. The undoped diamond film (Fig. 1(a)) mainly contains pyramid-shaped grains related to {111} facets. With the introduction of boron atoms, the majority of diamond grains (Figs. 1(b), (c)) show ridges and steps oriented parallel to one other, representing twin characteristic, which may result from the renucleation induced by B-doping [22]. As the B/C ratio increases to 4%, the grain size becomes small and crystal boundaries become vague. For the 6% boron-doped sample, which is in a considerably high doping level, the crystal shows an aggregation growth and the quality as well as continuity of diamond film

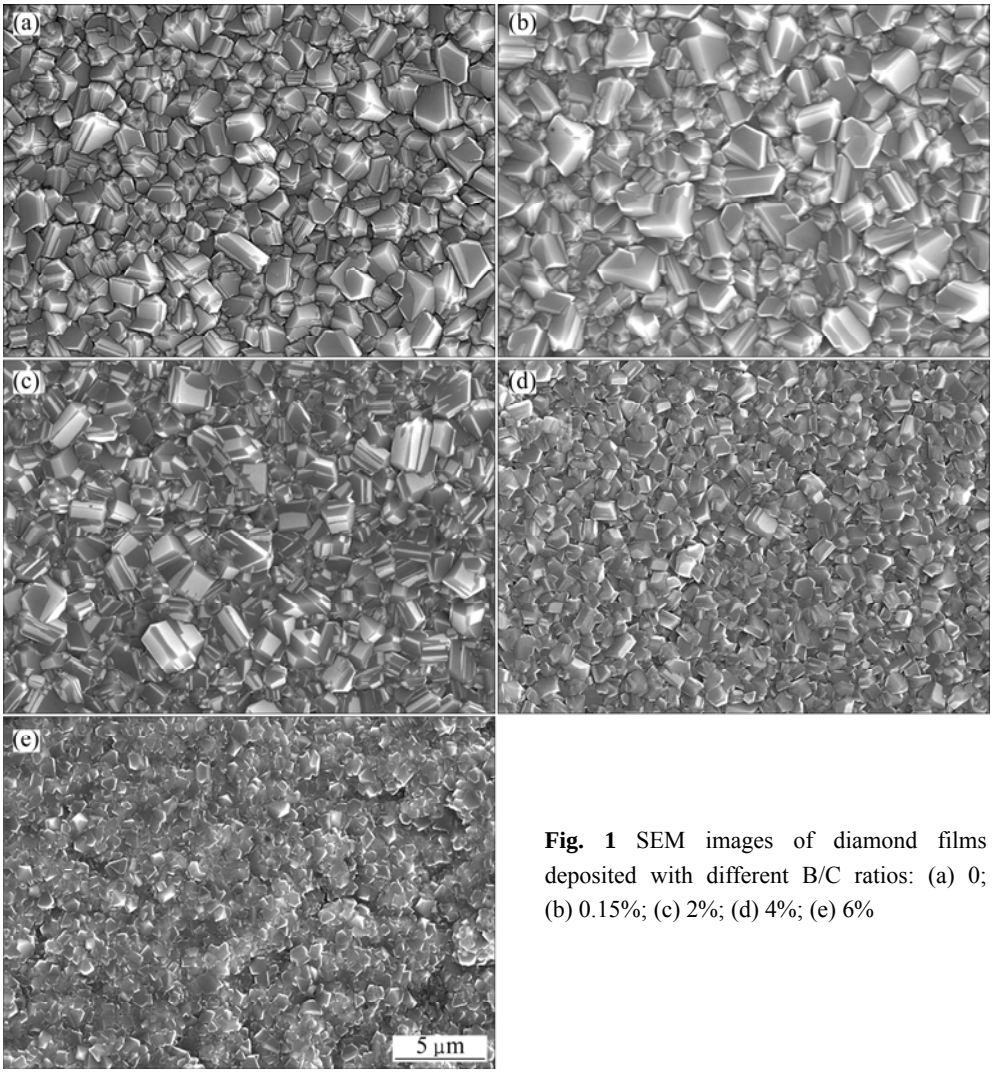

Fig. 1 SEM images of diamond films deposited with different B/C ratios: (a) 0; (b) 0.15%; (c) 2%; (d) 4%; (e) 6%

decreases sharply. One can conclude that the average diamond grain size observable on the film surface decreases with the increase of boron doping level. This result is in accordance with other works and can be explained by the enhanced nucleus formation due to the excess boron doping during the first step of growth [22,23].

Figure 2 shows the SEM cross-sectional morphologies of diamond films deposited for 6 h at different B/C ratios. It can be observed that a clear columnar structure of diamond films is formed. The thickness of the films decreases from 3.5 to 2.2 to 1.0 μm as the doping level increases from 0 (undoped film) to 2% to 6%. This phenomenon was observed by several authors [22,24] and indicates that incorporated boron atoms inhibit the growth of diamond film.

Figure 3 shows the representative atomic force microscopy (AFM) images (contact mode in air, over the 3 μm×3 μm area) and grain size distribution of the undoped and doped diamond films grown on Nb substrate. Clearly, the morphology of undoped diamond film is quite different from that of the doped diamond film. The undoped diamond film has a facet structure and the crystal size is evidently larger than the 6% boron-doped sample which shows a nodular structure. This is well consistent with the SEM images shown in Fig. 1. For undoped diamond film, the roughness is 63 nm, RMS roughness is 88 nm, and peak to peak separation is 692 nm. The corresponding R_a for 6% boron-doped sample is 31 nm, RMS roughness is 38 nm, and peak to peak separation is 235 nm.

Figure 4 shows the SEM images of Vickers indentation for 2% boron-doped sample under a load of 9.8 N. It can be seen that no obvious peelings or cracks are observed around the indentation. The microhardness test demonstrates the good adhesion between Nb substrate and as-grown BDD film and it is a prerequisite for the performance as a good electrode.

Figure 5(a) shows the Raman spectra of the comparatively light doped samples ranging from 0 to 0.45%. The result reveals that for 1500 samples, the diamond one phonon Raman peaks are symmetric and

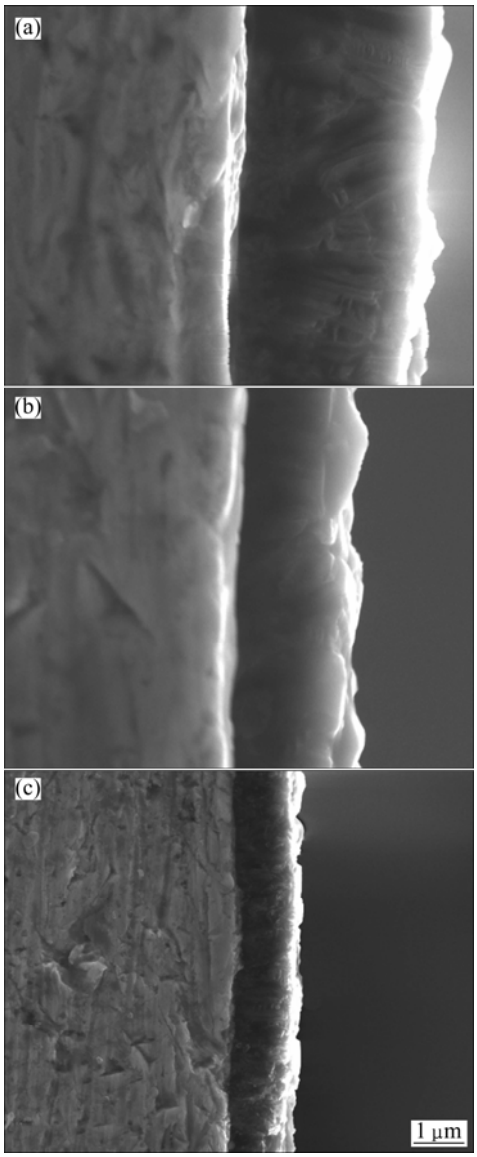

Fig. 2 Cross-sectional SEM images of diamond films deposited at different B/C ratios: (a) 0; (b) 2%; (c) 6%

narrow, indicating a very moderate boron-doping level [25]. With the increase of B content, the 1332 cm^{-1} peak becomes asymmetric with an upward shift in intensity on the high wave number side of the peak, which can be attributed to the Fano-type interference between the discrete phonon state and an electronic continuum [25,26].

Figure 5(b) shows the Raman spectra for films deposited at high B/C ratios (0.75%−6%). There are several drastic changes compared with the light doped samples: 1) The 1332 cm^{-1} peak gradually downshifts to ~1305 cm^{-1} and broadens as the boron content increases; 2) The diamond peak is attenuated while two new peaks emerge near 1210 cm^{-1} and 490 cm^{-1}; 3) Very weak bands related to sp^2-carbon impurities in the 1500−1600 cm^{-1} region are observed.

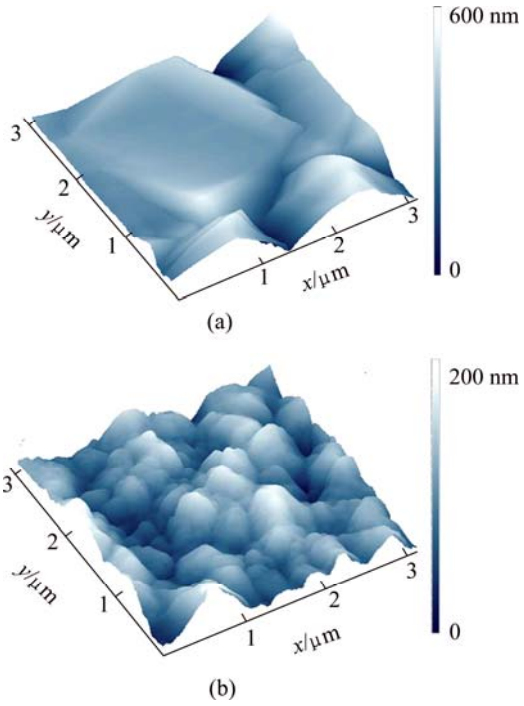

Fig. 3 AFM images of boron undoped diamond film surface (a) and heavily boron-doped diamond film surface grown at B/C ratio of 6% (b)

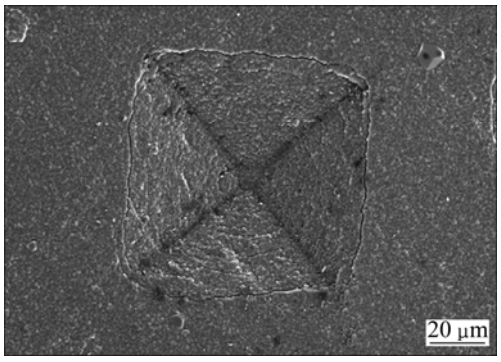

Fig. 4 Morphology of Vickers indentation on diamond film with 2% B/C ratio under load of 9.8 N

The downshift is mainly related to the Fano-effect which is formed at very high doping levels. The diamond peak broadening may result from the spread in phonon energy and/or phonon scattering by impurities and defects induced by B doping [27]. The origin of 500 cm^{-1} and 1200 cm^{-1} peaks is still uncertain now. Some authors have attributed these bands to scattering by local regions of microstructural disorder brought by the incorporation of high levels of substitutional boron [28]. Others ascribed that these bands to the two maxima in the phonon density of states (PDOS) and suggested that they may be connected with a relaxation of the wave-vector selection rules [29]. The peak 500 cm^{-1} can be used to estimate the B content ranging from 2×10^{20} to1×10^{22} cm^{-3} in BDD films after being fitted [30].

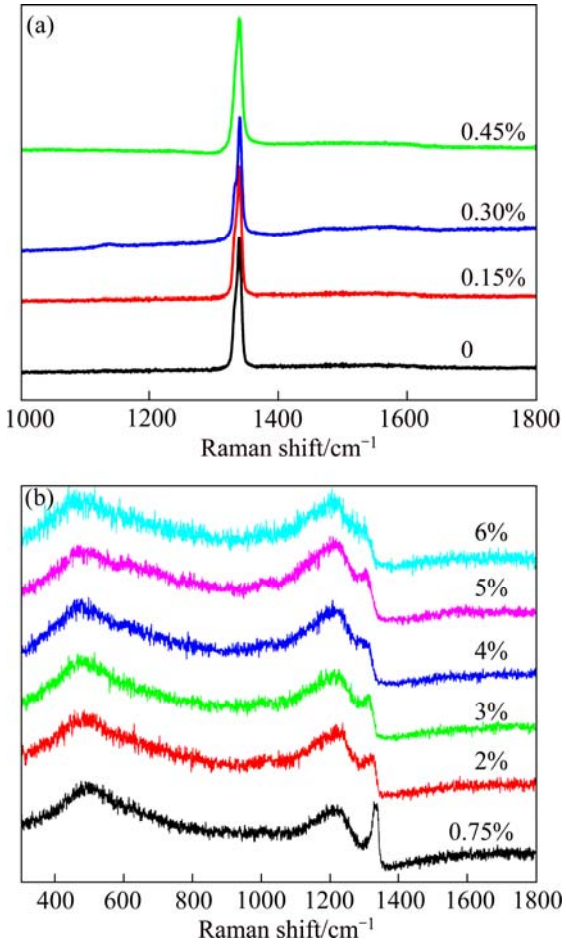

Fig. 5 Raman spectra of diamond films deposited at low (0−0.45%) (a) and high (0.75%−6%) (b) B_2H_6 concentrations

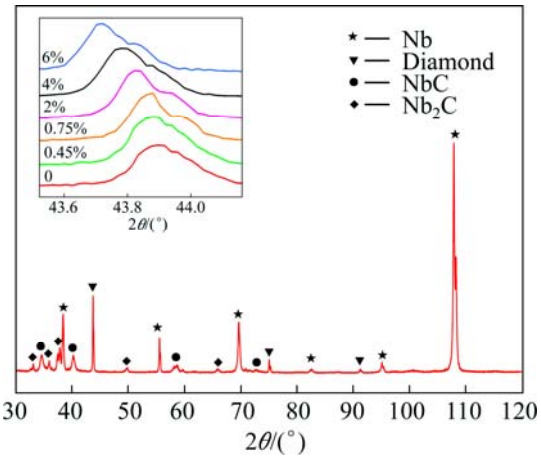

Fig. 6 XRD pattern of CVD diamond film deposited at B/C ratio of 2% (Inset shows magnification of (111) peaks of diamond films deposited at different doping levels)

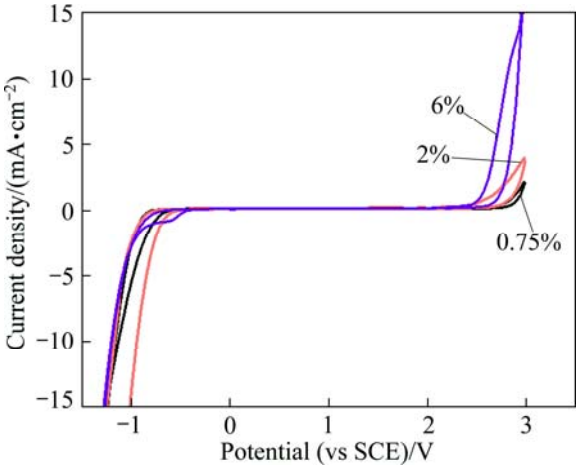

Fig. 7 Cyclic voltammetric curves for samples with different boron-doping concentrations in 1 mol/L H_2SO_4 solution

Figure 6 shows the XRD pattern of the 2% boron-doped sample. One can conclude that the peaks at 2θ=43.8° and 75.1°correspond to diffractions from diamond (111) and (220) planes. It is also found that the peaks at 2θ= 38.5°, 55.6°, 69.7°, 82.7°, 95.1°, 107.8° correspond to diffractions of Nb substrates. Furthermore, there are at least 14 peaks corresponding to the interlayer phase of Nb_2C and NbC. These metallic compounds are often required in order to protect the substrate against hydrogen in the deposition gas mixture and enhance the adhesion of the diamond film [3]. The insert figure shows the (111) peaks after magnification of diamond films deposited at different B_2H_6 concentrations. It is clear that the position of the (111) peaks downshifts with the increase of boron doping, which indicates an expansion of the lattice constant induced by the boron incorporation and hole concentration in the impurity bond of boron [31].

Cyclic valtammetry is nevertheless a useful and easy technique to evaluate the electrochemical behavior of the interface. Figure 7 shows the background cyclic voltammograms recorded for BDD electrodes doped with B/C ratios 0.75%, 2%, 6%, to measure the potential window width and background current in 1 mol/L H_2SO_4 solution. The typical values are depicted in Table 1. It can be seen from Fig. 7 and Table 1 that the potential window is the widest when the B/C ratio is relatively small, with a value of 3.8 V. The background currents for all electrodes are 1−2 order lower than freshly polished glassy carbon of the same geometric area, maintaining around 10^{-6} A, which means that there are no pinholes in the film. When the boron doping level is too high, the film will have more grain boundaries containing sp^2-related carbon impurities exposed and possess a higher density of electronic states. Hence, the 6% boron-doped sample has the narrowest potential window and highest background current among the moderate doping samples.

Table 1 Cyclic voltammetric data for samples with different boron-doping levels

B/C ratio/%	Potential window/V	Background current/μA	ΔEp (at 50 mV/s)/mV	J (at 50 mV/s)/(μA·cm^{-2})
0.75	−1.0−2.8 (3.8)	5	544	850
2	−1.0−2.8 (3.8)	6	119	1870
6	− 0.7−2.5 (3.2)	9	116	1910

The redox system of $Fe(CN)_6^{3-/4-}$ proceeds by an inner-sphere electron-transfer pathway with the electrode kinetics quite sensitive to surface cleanliness and the fraction of exposed edge plane on sp^2-bonded carbon, as well as the density of electronic states near the formal potential. Figure 8(a) shows the CV curves for an aqueous solution of 10 mmol/L $Fe(CN)_6^{3-/4-}$ in 0.1 mol/L KCl at undoped diamond electrode. No obvious anodic and cathodic peaks are observed and the background current is very small. Figures 8(b)−(d) show the CV curves for BDD without any conventional surface pretreatment. We can see the symmetrical redox couple peaks associated with the oxidation and reduction of the ferricyanide-ferrocyanide couple at the diamond film−solution interface. The oxidation peak current for the three electrode samples varies linearly from 50 mV/s to 250 mV/s, indicating that the reactions are controlled by semi-infinite linear diffusion of reactants to the electrode surface. Anodic to cathodic peak potential difference ΔE_p and oxidation current density J are also listed in Table1. For 0.75% boron-doped sample, because of the low density of electronic states, ΔE_p is considerably large (544 mV) while J is the smallest, revealing a slow redox reaction rate. ΔE_p values for 2% and 6% boron-doped samples obviously decrease but are much greater than 59 mV expected for an electrode reaction showing true electrochemical reversibility. Since the BDD electrodes utilized were exposed to the laboratory atmosphere for several weeks and the CV curves in $Fe(CN)_6^{3-/4-}$ were tested after analysis in the acid solution, the BDD films may change from a hydrogen to an oxygen surface termination. ΔE_p is very sensitive to the surface termination and the smallest ΔE_p can be observed on the clean, hydrogen-terminated surface [15].

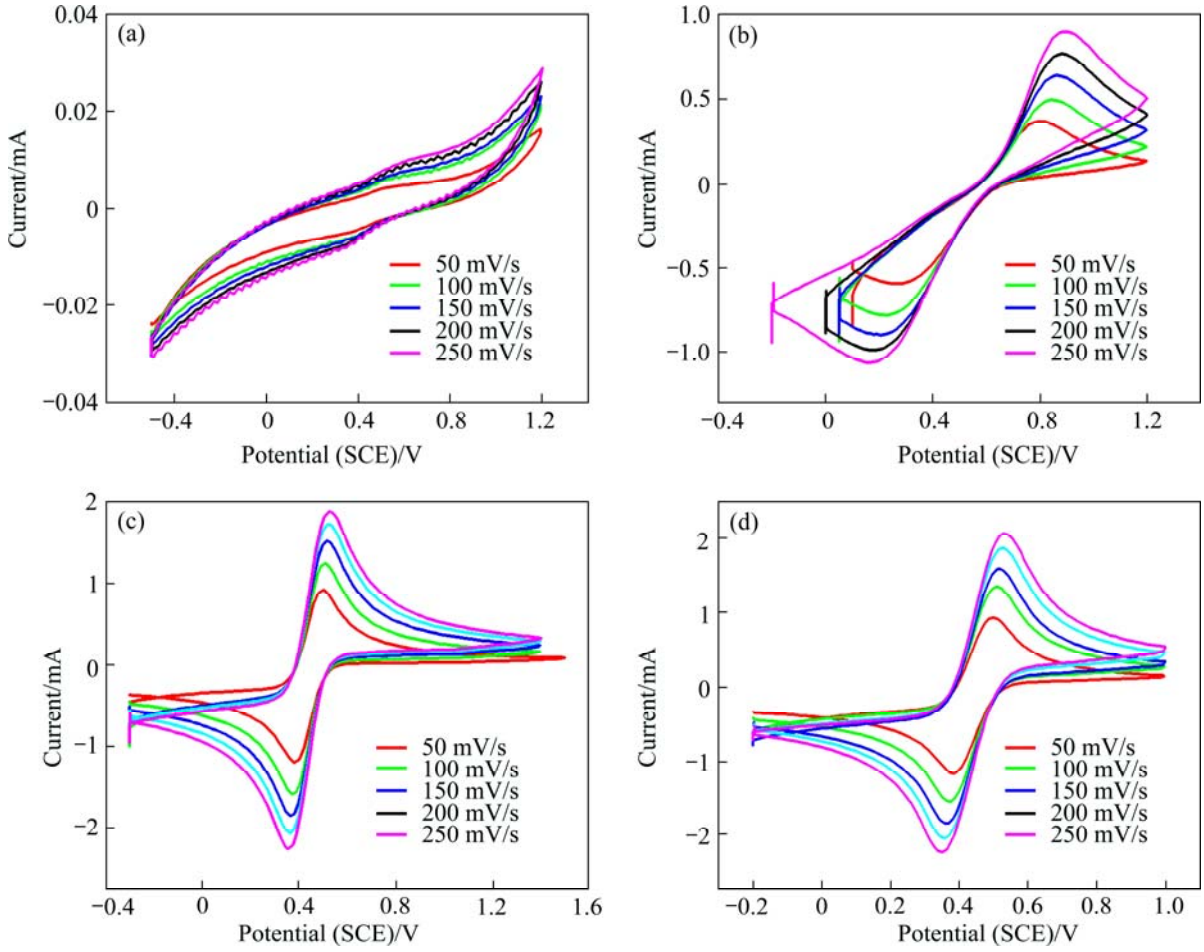

Fig. 8 Cyclic voltammetric curves for 0% (a), 0.75% (b), 2% (c), 6% (d) boron-doped samples in 10 mmol/L $Fe(CN)_6^{3-/4-}$+0.1 mol/L KCl (Scaning rate: 50−250 mV/s)

4 Conclusions

1) The grain size and growth rate of the coatings decrease whereas the lattice constant of diamond expands with increasing B_2H_6 levels in the gas phase, offering similar evolutions in comparison with diamond films deposited on Si substrate.

2) When subjected to cyclic voltammetric measurement against 1 mol/L H_2SO_4 solution, the boron-doped diamond films show wide working potential window (3.2−3.8 V) and low background current (5−9 μA) without any pretreatment.

3) Analysis of the ferrocyanide-ferrricyanide couple at the BDD electrodes shows some extent of electrochemical reversibility. The oxidation peak current for all BDD electrodes varies linearly with scaning rate in the redox system, which indicates that the reactions are controlled by diffusive mass transport. The redox reaction rate increases with the increase of boron doping level due to the enhanced density of electronic states.

4) The sample deposited with an intermediate boron content (2% B/C ratio) has the wider potential window and relatively low background current as well as fast redox reaction rate in H_2SO_4 solution and $KFe(CN)_6$ redox system compared with other doping level electrodes.

References

[1] VOLPE P N, PERNOT J, MURET P, OMNES F. High hole mobility in boron doped diamond for power device applications [J]. Appl Phys Lett, 2009, 94: 092102.

[2] TEII K, NAKASHIMA M. Synthesis and field emission properties of nanocrystalline diamond/carbon nanowall composite films [J]. Appl Phys Lett, 2010, 96: 023112.

[3] LUONG J H T, MALE K B, GLENNON J D. Boron-doped diamond electrode: Synthesis, characterization, functionalization and analytical applications [J]. Analyst, 2009, 134: 1965−1979.

[4] COLLINS A T, DEAN P J, LIGHTOWLERS E C, SHERMAN W F. Acceptor-impurity infrared absorption in semiconducting synthetic diamond [J]. Physical Review A, 1965, 140: 1272.

[5] TAKANO Y, NAGAO M, SAKAGUCHI I, TACHIKI M, HATANO T, KOBAYASHI K, UMEZAMA H, KAWARADE H. Superconductivity in diamond thin films well above liquid helium temperature [J]. Appl Phys Lett, 2004, 85: 2851−2853.

[6] KAWANO A, ISHIWATA H, IRIYAMA S, OKADA R, YAMAGUCHI T, TAKANO Y, KAWARADA H. Superconductor-to-insulator transition in boron-doped diamond films grown using chemical vapor deposition [J]. Physical Review B, 2010, 82: 085318.

[7] TROUILLON R, O'HARE D. Comparison of glassy carbon and boron doped diamond electrodes: Resistance to biofouling [J]. Electrochimica Acta, 2010, 55: 6586−6595.

[8] OLIVEIRA S C B, OLIVEIRA-BRETT A M. Boron doped diamond electrode pre-treatments effect on the electrochemical oxidation of dsDNA, DNA bases, nucleotides, homopolynucleotides and biomarker 8-oxoguanine [J]. Journal of Electroanalytical Chemistry, 2010, 648: 60−66.

[9] CANIZARES P, ARCIS M, SAEZ C, RODRIGO M A. Electrochemical synthesis of ferrate using boron doped diamond anodes [J]. Electrochemistry Communications, 2007, 9: 2286−2290.

[10] ZHANG C Y, WANG J L, ZHOU H F, FU D G, GU Z Z. Anodic treatment of acrylic fiber manufacturing wastewater with boron-doped diamond electrode: A statistical approach [J]. Chemical Engineering Journal, 2010, 161: 93−98.

[11] ACTIS P, DENOYELLE A, BOUKHERROUB R, SZUNERITS S. Influence of the surface termination on the electrochemical properties of boron-doped diamond (BDD) interfaces [J]. Electrochemistry Communications, 2008, 10: 402−406.

[12] WANG S, SWOPE V M, BULTER J E, FEYGELSON T, SWAIN G M. The structural and electrochemical properties of boron-doped nanocrystalline diamond thin-film electrodes grown from Ar-rich and H_2-rich source gases [J]. Diamond and Related Materials, 2009, 18: 669−677.

[13] FISCHER A E, SHOW Y, SWAIN G M. Electrochemical performance of diamond thin-film electrodes from different commercial sources [J]. Analytical Chemistry, 2004, 76: 2553−2560.

[14] WANG S H, SWAIN G M. Spatially heterogeneous electrical and electrochemical properties of hydrogen-terminated boron-doped nanocrystalline diamond thin film deposited from an argon-rich CH4/H_2/Ar/B2H6 source gas mixture [J]. Journal of Physical Chemistry C, 2007, 111: 3986−3995.

[15] GRANGER M C, WITEK M, XU J S, WANG J, HUPERT M, HANKS A, KOPPANG M, BUTLER M, LUCAZEAU G, MERMOUX M, STROJEK J, SUAIN G. Standard electrochemical behavior of high-quality, boron-doped polycrystalline diamond thin-film electrodes [J]. Analytical Chemistry, 2000, 72: 3793−3804.

[16] NOWAK I, ZIOLEK M. Niobium compounds: Preparation, characterization, and application in heterogeneous catalysis [J]. Chemical Reviews, 1999, 99: 3603−3624.

[17] van HEGE K, VERHAEGE M, VERSTRAETE W. Indirect electrochemical oxidation of reverse osmosis membrane concentrates at boron-doped diamond electrodes [J]. Electrochemistry Communications, 2002, 4: 296−300.

[18] NDAO A N, ZENIA F, DENEUVILLE A, BERNARD M, LEVY-CLEMENT C. Effect of boron concentration on the electrochemical reduction of nitrates on polycrystalline diamond electrodes [J]. Diamond and Related Materials, 2000, 9: 1175−1180.

[19] JIA F C, BAI Y Z, QU F, ZHAO J J, ZHUANG C Q, JIANG X. Effect of B/C ratio on the physical properties of highly boron-doped diamond films [J]. Vacuum, 2010, 84: 930−934.

[20] YU Z, KARLSSON U, FLODSTROM A. Influence of oxygen and nitrogen on the growth of hot-filament chemical vapor deposited diamond films [J]. Thin Solid Films, 1999, 342: 74−82.

[21] WANG S G, ZHANG Q, YOON S F, AHN J, WANG Q, YANG D J, HUANG Q F, RUSLI, TANG W Z, LU F X. CVD diamond nucleation enhanced by ultrasonic pretreatment using diamond and mixture of diamond and TaC powders [J]. Diamond and Related Materials, 2002, 11: 1683−1689.

[22] RAMAMURTI R, BECKER M, SCHUELKE T, GROTJOHN T, REINHARD D, SWAIN G, ASMUSSEN J. Boron doped diamond deposited by microwave plasma-assisted CVD at low and high pressures [J]. Diamond and Related Materials, 2008, 17: 481−485.

[23] GONCALVES J A N, SANDONATO G M, IHA K. Characterization of boron doped CVD diamond films by Raman spectroscopy and X-ray diffractometry [J]. Diamond and Related Materials, 2002, 11: 1578−1583.

[24] BRUNET F, GERMI P, PERNET M. Microstructural study of boron doped diamond films by X-ray diffraction profiles analysis [J]. Thin Solid Films, 1998, 322: 143−147.

[25] AGER III J W, WALUKIEWICZ W, MCCLUSKEY M, PLANO M

A, LANDSTRASS M I. Fano interference of the Raman phonon in heavily boron-doped diamond films grown by chemical vapor deposition [J]. Appl Phys Lett, 1995, 66: 616−618.
[26] PRUVOST F, DENEUVILLE A. Analysis of the Fano in diamond [J]. Diamond and Related Materials, 2001, 10: 531−535.
[27] BERGMAN L, NEMANICH R J. Raman and photoluminescence analysis of stress state and impurity distribution in diamond thin films [J]. Journal of Applied Physics, 1995, 78: 6709−6719.
[28] BERNARD M, BARON C, DENEUVILLE A. About the origin of the low wave number structures of the Raman spectra of heavily boron doped diamond films [J]. Diamond and Related Materials, 2004, 13: 896−899.
[29] MAY P W, ASHFOLD M N R, MANKELEVICH Y A. Microcrystalline, nanocrystalline, and ultrananocrystalline diamond chemical vapor deposition: Experiment and modeling of the factors controlling growth rate, nucleation, and crystal size [J]. Journal of Applied Physics, 2007, 101: 053115.
[30] BERNARD M, DENEUVILLE A, MURET P. Non-destructive determination of the boron concentration of heavily doped metallic diamond thin films from Raman spectroscopy [J]. Diamond and Related Materials, 2004, 13: 282−286.
[31] BRUNET F, GERMI P, PERNET M, DENEUVILLE A, GHEERAERT E, LAUGIER F, BURDIN M, ROLLAND G. The effect of boron doping on the lattice parameter of homoepitaxial diamond films [J]. Diamond and Related Materials, 1998, 7: 869−873.

铌基体上硼掺杂金刚石薄膜电极的制备、表征和电化学性能

余志明[1,2]，王 健[1]，魏秋平[1,2]，孟令聪[1]，郝诗梦[1]，龙 芬[1]

1. 中南大学 材料科学与工程学院，长沙 410083；
2. 中南大学 粉末冶金国家重点实验室，长沙 410083

摘 要：采用热丝化学气相沉积法在铌基体上制备一系列硼掺杂金刚石薄膜电极，并通过扫描电子显微镜、激光拉曼光谱、X 射线衍射、显微硬度和电化学分析等手段研究沉积所得样品中 B/C 比对薄膜的形貌、生长速率、化学键结构、物相组成和电化学性能的影响。结果表明：金刚石的平均晶粒尺寸和生长速率随着 B/C 比的增加而减小；金刚石薄膜在 9.8 N 载荷下的维氏显微压痕测试中表现出优异的结合强度；相对于其他掺杂水平的样品，B/C 比为 2%的 BDD 电极具有更宽的电势窗口和更低的背景电流以及在 H_2SO_4 和 $KFe(CN)_6$ 溶液中更快的氧化还原反应速率。

关键词：金刚石薄膜；热丝化学气相沉积；硼掺杂；电化学性能；铌基体；电极

(Edited by Xiang-qun LI)